Impact of Motion and Channel Parameters on the Estimation of Transmitter Position in Robotic Networks

Mehrzad Malmirchegini, Alireza Ghaffarkhah and Yasamin Mostofi

***Abstract*—In this paper we study the impact of the motion of a mobile robot as well as the underlying parameters of the channel on the estimation of the transmitter position in a networked robotic operation. We consider the case that the robot gathers a number of received signal strength (RSS) measurements from a fixed transmitter along its trajectory and use them to estimate the position of the transmitter. We first mathematically characterize two metrics for the estimation performance of the transmitter position: 1) the Cramer-Rao lower bound (CRLB) and 2) the error covariance matrix of a least square (LS) estimator. We then mathematically analyze the impact of the positions of the channel measurements as well as the underlying channel parameters, such as shadowing power, correlation distance, multipath power, and path loss slope, on each metric individually. Motivated by our analysis, we then utilize a motion planning strategy to improve the estimation quality of the transmitter position. Our simulation results confirm our theoretical analysis.**

I. Introduction

The problem of localizing the transmitter in a wireless sensor/robotic network is a well-known problem and has a variety of potential applications such as connectivity maintenance, robotic routers, interference cancelation, and emergency response [1]–[3]. Generally, two types of transmitter position estimation techniques have been proposed in the literature: direct positioning and two-step positioning. Direct positioning refers to the direct assessment of the transmitter position from the signals traveled between the nodes [4]. On the other hand, in two-step positioning, certain signal parameters, such as angle of arrival (AOA), time of arrival (TOA), or received signal strength (RSS), are first extracted. Then, geometric or statistical approaches are used to estimate the transmitter position. Among the various parameters, RSS is used more often as it is readily available in almost any low-cost wireless hardware. Therefore, in this paper we focus on RSS-based localization. In [5], authors considered the ray-tracing model for a specific propagation environment and devise a motion planning strategy, which routes a mobile agent to the transmitter. In [6], authors considered motion planning for model-based localization of a transmitter. In [7], [8], we proposed a probabilistic framework to predict the spatial variations of the RSS, based on a small number of wireless channel measurements. More specifically, we analyzed the effects of the underlying channel parameters on channel prediction quality when the position of the transmitter is known.

In this paper, we focus on estimating the transmitter position based on a small number of RSS measurements. We utilize the realistic multi-scale probabilistic channel model of [7]–[9] and analyze the performance of the transmitter position estimation. Our main goal is to mathematically characterize the impact of the underlying channel parameters as well as the measurement positions on the estimation quality. We consider two performance metrics: the Cramer-Rao lower bound (CRLB) of the localization performance and the error covariance of a least square (LS) estimator. Motivated by our analysis, we then utilize a motion planning strategy to improve the estimation performance.

The rest of this paper is organized as follows. In Section II, we describe the probabilistic multi-scale model of wireless channels. In Section III and IV, we mathematically characterize the impact of the channel underlying parameters as well as sampling positions on the CRLB and the LS estimation error covariance respectively. Section V is then on motion planning for improving the estimation performance. We present our simulation results in Section VI, followed by the conclusions in Section VII.

II. System model

In wireless communication literature it is well-established that the RSS between a transmitter and a receiver can be modeled as a multi-scale non-stationary random field with three major dynamics: path loss, shadowing and multipath fading [10]. Let $\Upsilon_{\text{dB}}(q)$ denote the RSS in dB, in the transmission from a fixed transmitter at position $q_b = [x_b, y_b]^T \in \mathcal{W}$ to a receiver at position $q \in \mathcal{W}$, where $\mathcal{W} \subset \mathbb{R}^2$ denotes a given workspace. We then have the following [10]:

$$\Upsilon_{\text{dB}}(q) = K_{\text{dB}} - 10n_{\text{PL}} \log_{10}\left(\|q - q_b\|\right) + \xi(q) + \omega(q),$$

where K_{dB} and n_{PL} are the path loss parameters, and $\xi(q)$ and $\omega(q)$ are zero-mean random variables that represent the effects of shadowing and multipath components in dB, respectively. In the communication literature, the distribution and spatial correlation of $\xi(q)$ and $\omega(q)$ are typically found based on empirical data [10]. In this paper, we consider a Gaussian distribution for $\xi(q)$, with an exponential correlation, and an uncorrelated Gaussian distribution for $\omega(q)$. The justification of this model, using empirical data, can be found in [7], [8], [11].

Consider the case where the RSS to a fixed transmitter is sparsely measured by a mobile robot along its trajectory at a set of positions $\mathcal{Q} = \{q_1, q_2, \cdots, q_k\} \subset \mathcal{W}$, where

Mehrzad Malmirchegini and Alireza Ghaffarkhah are with the Department of Electrical and Computer Engineering, University of New Mexico, Albuquerque, NM 87113, USA email: {mehrzad,alinem}@ece.unm.edu. Yasamin Mostofi is with the Department of Electrical and Computer Engineering, University of California, Santa Barbara, CA 93106, USA email: ymostofi@ece.ucsb.edu.

This work is supported in part by ARO CTA MAST project # W911NF-08-2-0004.

$q_i = [x_i, y_i]^T$ denotes the position of the ith RSS measurement. Let $D_{\mathcal{Q}}(q_b)$ and $Z_{\mathcal{Q}}$ denote the corresponding distance vector to the transmitter in dB and the stacked vector of the RSS measurements, respectively: $D_{\mathcal{Q}}(q_b) = \Big[10\log_{10}(\|q_1 - q_b\|), \cdots, 10\log_{10}(\|q_k - q_b\|)\Big]^T$ and $Z_{\mathcal{Q}} = [z_1, \cdots, z_k]^T \in \mathbb{R}^k$. We have,

$$Z_{\mathcal{Q}} = \underbrace{\big[1_k \quad -D_{\mathcal{Q}}(q_b)\big]}_{H_{\mathcal{Q}}(q_b)}\theta + \Xi_{\mathcal{Q}} + \Omega_{\mathcal{Q}}, \tag{1}$$

where 1_k denotes the k-dimensional vector of ones, $\theta = [K_{\text{dB}} \quad n_{\text{PL}}]^T$, $\Xi_{\mathcal{Q}} = \big[\xi(q_1), \cdots, \xi(q_k)\big]^T$ and $\Omega_{\mathcal{Q}} = \big[\omega(q_1), \cdots, \omega(q_k)\big]^T$. Based on the exponentially correlated Gaussian distribution for $\xi(q)$, $\Xi_{\mathcal{Q}}$ is a zero-mean Gaussian random vector with covariance matrix $\alpha R_{\text{norm},\mathcal{Q}}$, where $\big[R_{\text{norm},\mathcal{Q}}\big]_{i,j} = e^{-\|q_i - q_j\|/\beta}$, for $q_i, q_j \in \mathcal{Q}$, α is the power of the shadowing component in dB, and β is its *correlation distance* [7]. Similarly, based on the uncorrelated Gaussian distribution for $\omega(q)$, $\Omega_{\mathcal{Q}}$ is a zero-mean Gaussian vector with the covariance matrix $\sigma^2 I_k$, where I_k is the k-dimensional identity matrix and σ^2 denotes the power of multipath fading in dB. Consequently, the summation of shadowing and multipath terms, i.e., $\Xi_{\mathcal{Q}} + \Omega_{\mathcal{Q}}$, is also a zero-mean Gaussian vector with covariance matrix $R_{\text{tot},\mathcal{Q}} = \alpha R_{\text{norm},\mathcal{Q}} + \sigma^2 I_k$.

III. Cramer-Rao Lower Bound (CRLB) for the Estimation of the Transmitter Position

Conditioned on the channel underlying parameters, the ML estimation of q_b is given as follows:

$$\begin{aligned}\hat{q}_{b,\text{ML}} &= \text{argmax}_{q_b}\text{Prob}\big(Z_{\mathcal{Q}}\big|q_b, \theta, \alpha, \beta, \sigma\big) \\ &= \text{argmin}_{q_b}\big(Z_{\mathcal{Q}} - H_{\mathcal{Q}}(q_b)\theta\big)^T R^{-1}_{\text{tot},\mathcal{Q}}\big(Z_{\mathcal{Q}} - H_{\mathcal{Q}}(q_b)\theta\big).\end{aligned} \tag{2}$$

Finding a closed-form expression for the transmitter position and the corresponding estimation error variance based on this expression is, however, very challenging. Instead, we calculate the inverse of *Fisher information*, which is the Cramer-Rao lower bound (CRLB) on the covariance of any unbiased estimator of the transmitter position, and use that as a measure of uncertainty [1]. It can be confirmed that for any unbiased estimate of the transmitter position, the estimation error covariance is lower bounded by its CRLB as follows:

$$\begin{aligned}&\mathbb{E}\big\{(\hat{q}_b - q_b)(\hat{q}_b - q_b)^T\big\} \succeq \\ &\frac{1}{n_{\text{PL}}^2}\begin{bmatrix} D^T_{\mathcal{Q},x_b}R^{-1}_{\text{tot},\mathcal{Q}}D_{\mathcal{Q},x_b} & D^T_{\mathcal{Q},x_b}R^{-1}_{\text{tot},\mathcal{Q}}D_{\mathcal{Q},y_b} \\ D^T_{\mathcal{Q},x_b}R^{-1}_{\text{tot},\mathcal{Q}}D_{\mathcal{Q},y_b} & D^T_{\mathcal{Q},y_b}R^{-1}_{\text{tot},\mathcal{Q}}D_{\mathcal{Q},y_b}\end{bmatrix}^{-1} \triangleq J^{-1}(\mathcal{Q}, q_b),\end{aligned} \tag{3}$$

where $J(\mathcal{Q}, q_b)$ denotes the Fisher information, $D_{\mathcal{Q},x_b} \triangleq \frac{d}{dx_b}D_{\mathcal{Q}}$, $D_{\mathcal{Q},y_b} \triangleq \frac{d}{dy_b}D_{\mathcal{Q}}$ and $\hat{q}_b$ represents any unbiased estimation of q_b. Next, we mathematically analyze the impact of the underlying channel parameters as well as channel measurement positions on the CRLB. Such a characterization provides a fundamental understanding on how different environmentalists, in terms of the underlying channel parameters, affect the estimation quality of the transmitter position. In Section IV, we then directly characterize the impact of the underlying parameters on the LS estimation of the transmitter position. Our CRLB characterization is also a lower bound for the LS estimation of Section IV and therefore can serve as a benchmark.

[1]Note that in this paper we use the terms "Cramer-Rao lower bound" and "inverse of Fisher information" interchangeably.

A. Impact of the Underlying Channel Parameters and Sampling Positions on CRLB

The next theorem characterizes the impact of the channel parameters on $J^{-1}(\mathcal{Q}, q_b)$:

Theorem III.1. *We have the following properties for the CRLB of (3): 1) $J^{-1}(\mathcal{Q}, q_b)$ does not depend on K_{dB} and is a decreasing function of n_{PL}; 2) for the 1D scenario, $J^{-1}(\mathcal{Q}, q_b)$ is an increasing function of α and σ^2, for $\alpha, \sigma^2 \in [0, \infty)$ and an invertible $R_{norm,\mathcal{Q}}$; 3) for the 1D scenario, $J^{-1}(\mathcal{Q}, q_b)$ is not a decreasing (or increasing) function of β for every $\mathcal{Q}$; 4) for the 1D scenario and $\frac{\sigma^2}{\alpha} \ll 1$, we have $J^{-1}(\mathcal{Q}, q_b)\big|_{\beta=\infty} \leq J^{-1}(\mathcal{Q}, q_b)\big|_{\beta=0}$.*

Proof: The first property is clear from the form of $J^{-1}(\mathcal{Q}, q_b)$. To prove the second property, we use the fact that for a 1D scenario $J^{-1}(\mathcal{Q}, q_b) = \frac{1}{n_{\text{PL}}^2}\Big(D^T_{\mathcal{Q},x_b}R^{-1}_{\text{tot},\mathcal{Q}}D_{\mathcal{Q},x_b}\Big)^{-1}$. We have $\frac{d}{d\sigma^2}D^T_{\mathcal{Q},x_b}R^{-1}_{\text{tot},\mathcal{Q}}D_{\mathcal{Q},x_b} = -D^T_{\mathcal{Q},x_b}R^{-2}_{\text{tot},\mathcal{Q}}D_{\mathcal{Q},x_b} < 0$. Therefore, $J^{-1}(\mathcal{Q}, q_b)$ is an increasing function of σ^2. We also have, $\frac{d}{d\alpha}D^T_{\mathcal{Q},x_b}R^{-1}_{\text{tot},\mathcal{Q}}D_{\mathcal{Q},x_b} = -D^T_{\mathcal{Q},x_b}R^{-1}_{\text{tot},\mathcal{Q}}R_{\text{norm},\mathcal{Q}}R^{-1}_{\text{tot},\mathcal{Q}}D_{\mathcal{Q},x_b} < 0$, which implies that $J^{-1}(\mathcal{Q}, q_b)$ is an increasing function of α. Next we prove the third property. We have $D_{\mathcal{Q},x_b} = \frac{10}{\ln(10)}[\frac{1}{x_1 - x_b}, \cdots, \frac{1}{x_k - x_b}]^T$. We consider two extreme cases of $\beta = 0$ and $\beta = \infty$. After some lines of derivations, we can show that

$$\begin{aligned}&D^T_{\mathcal{Q},x_b}R^{-1}_{\text{tot},\mathcal{Q}}\big|_{\beta=\infty}D_{\mathcal{Q},x_b} - D^T_{\mathcal{Q},x_b}R^{-1}_{\text{tot},\mathcal{Q}}\big|_{\beta=0}D_{\mathcal{Q},x_b} \\ &= D^T_{\mathcal{Q},x_b}\left[\frac{\alpha}{\sigma^2(\alpha+\sigma^2)}I_k - \frac{\alpha}{\sigma^2(k\alpha+\sigma^2)}1_k 1_k^T\right]D_{\mathcal{Q},x_b}.\end{aligned} \tag{4}$$

It can be easily confirmed that the matrix $\frac{\alpha}{\sigma^2(\alpha+\sigma^2)}I_k - \frac{\alpha}{\sigma^2(k\alpha+\sigma^2)}1_k 1_k^T$ is indefinite for $\alpha \neq 0$. Since $D_{\mathcal{Q},x_b}$ spans $\mathbb{R}^k$, the left hand side of (4) can be positive or negative, depending on $\mathcal{Q}$. This proves the third property. To prove the forth property, it suffices to show that $\frac{\left(1_k^T D^T_{\mathcal{Q},x_b}\right)^2}{\|D_{\mathcal{Q},x_b}\|^2} \leq \frac{k+\frac{\sigma^2}{\alpha}}{1+\frac{\sigma^2}{\alpha}} \approx k$ for $\frac{\sigma^2}{\alpha} \ll 1$. This is equivalent to showing that $D^T_{\mathcal{Q},x_b}(kI_k - 1_k 1_k^T)D_{\mathcal{Q},x_b} \geq 0$, which is always true since $kI_k - 1_k 1_k^T$ is a positive-semidefinite matrix. ■

We next investigate the impact of the channel measurement positions on $J^{-1}(\mathcal{Q}, q_b)$. Since the mathematical analysis for a general distribution of positions is considerably challenging, we limit our analysis to the case where our channel measurements are far enough from transmitter position.

Theorem III.2. *Without loss of generality, consider the case that the transmitter is located at the origin. Assume there exists*

$q^* = [\rho\cos(\phi), \rho\sin(\phi)]^T \in \mathcal{W}$ *such that* $\|q_i - q^*\| \ll \rho\ \forall i$. *Then, if* $\beta \to 0$ *(uncorrelated channel),* $\mathrm{trace}\{J^{-1}(\mathcal{Q}, q_b)\}$ *is an increasing function of* ρ *for sufficiently large* ρ.

Proof: When $\beta \to 0$, we have $\mathrm{trace}\{J^{-1}(\mathcal{Q}, q_b)\} = \frac{\alpha+\sigma^2}{n_{\mathrm{PL}}^2} \frac{\|D_{\mathcal{Q},x_b}\|^2 + \|D_{\mathcal{Q},y_b}\|^2}{\|D_{\mathcal{Q},x_b}\|^2\|D_{\mathcal{Q},y_b}\|^2 - (D_{\mathcal{Q},x_b}^T D_{\mathcal{Q},y_b})^2}$. Since $\|q_i - q^*\| \ll \rho$, we have $D_{\mathcal{Q},x_b} \approx \frac{10}{\ln(10)\rho^2}[x_1, \cdots, x_k]^T$ and $D_{\mathcal{Q},y_b} \approx \frac{10}{\ln(10)\rho^2}[y_1, \cdots, y_k]^T$. Assume (ρ_i, ϕ_i) denotes the polar representation of the displacement of q_i with respect to q^*. We then have $x_i = \rho\cos(\phi) + \rho_i\cos(\phi_i)$ and $y_i = \rho\sin(\phi) + \rho_i\sin(\phi_i)$. Then $\|D_{\mathcal{Q},x_b}\|^2 = \frac{\zeta^2}{\rho^4}\Big[k\cos^2(\phi)\rho^2 + 2\cos(\phi)\sum_i \rho_i\cos(\phi_i)\rho + \sum_i \rho_i^2\cos^2(\phi_i)\Big]$, $\|D_{\mathcal{Q},y_b}\|^2 = \frac{\zeta^2}{\rho^4}\Big[k\sin^2(\phi)\rho^2 + 2\sin(\phi)\sum_i \rho_i\sin(\phi_i)\rho + \sum_i \rho_i^2\sin^2(\phi_i)\Big]$, and $D_{\mathcal{Q},x_b}^T D_{\mathcal{Q},y_b} = \frac{\zeta^2}{\rho^4}\Big[k\sin(\phi)\cos(\phi)\rho^2 + \sum_i \rho_i\big(\sin(\phi)\cos(\phi_i) + \cos(\phi)\sin(\phi_i)\big)\rho + \sum_i \rho_i^2\sin(\phi_i)\cos(\phi_i)\Big]$, where $\zeta \triangleq \frac{10}{\ln(10)}$. After some lines of derivations, it can then be shown that

$$\frac{\|D_{\mathcal{Q},x}\|^2 + \|D_{\mathcal{Q},y}\|^2}{\|D_{\mathcal{Q},x}\|^2\|D_{\mathcal{Q},y}\|^2 - \big(D_{\mathcal{Q},x}^T D_{\mathcal{Q},y}\big)^2} = \frac{\rho^4\big(k\rho^2 + f_1(\rho)\big)/\zeta^2}{\Big(k\sum_i \rho_i^2\sin^2(\phi - \phi_i) - \big[\sum_i \rho_i\sin(\phi - \phi_i)\big]^2\Big)\rho^2 + f_2(\rho)}, \tag{5}$$

where $f_1(\rho)$ and $f_2(\rho)$ are first-order polynomials of ρ. Define $\psi \triangleq [\rho_1\sin(\phi - \phi_1), \cdots, \rho_k\sin(\phi - \phi_k)]^T$. We then have $k\sum_i \rho_i^2\sin^2(\phi - \phi_i) - \big[\sum_i \rho_i\sin(\phi - \phi_i)\big]^2 = \psi^T(kI_k - 1_k 1_k^T)\psi \geq 0$, since $kI_k - 1_k 1_k^T$ is positive-semidefinite. Therefore, for sufficiently large values of ρ, $\mathrm{trace}\{J^{-1}(\mathcal{Q}, q_b)\}$ is an increasing function of ρ. ∎

Theorem III.2 indicates that if $\mathrm{trace}\{J^{-1}(\mathcal{Q}, q_b)\}$ is chosen as the objective function for motion planning, the optimal trajectory tends to move the robot towards the transmitter, when the channel measurements are far from the transmitter and channel is spatially uncorrelated. We use this property when designing our motion planning strategy in Section V.

IV. Least Square(LS) Estimation of the Transmitter Position

In this section, we utilize an unbiased LS estimator for the transmitter position based on a method called *lateration* [12]–[14]. This estimator is less computationally expensive, as compared to ML estimator, and is more useful for practical purposes. Furthermore, in this approach there exists a closed-form solution for the estimated position and its estimation error covariance, which makes it more suitable for motion planning purposes. Let $\hat{d}_i$, for $1 \leq i \leq k$, denote an estimate of the distance of the ith channel measurement to the transmitter. Define $U \triangleq [x_2 - x_1, \cdots, x_k - x_1]^T$, $V \triangleq [y_2 - y_1, \cdots, y_k - y_1]^T$, $A \triangleq 2[U,\ V]$ and $b \triangleq \big[x_2^2 - x_1^2 + y_2^2 - y_1^2, \cdots, x_k^2 - x_1^2 + y_k^2 - y_1^2\big]^T - \big[\hat{d}_2^2 - \hat{d}_1^2, \cdots, \hat{d}_k^2 - \hat{d}_1^2\big]^T$. In the lateration method, the LS estimate of the transmitter position is found by minimizing $\|Aq_b - b\|$ which results in

$$\hat{q}_{b,\mathrm{LS}} = (A^T A)^{-1} A^T b. \tag{6}$$

The necessary and sufficient condition for this estimator to be unbiased is $\mathbb{E}\{\hat{d}_i^2\} = d_i^2$, for all i. An estimate of d_i that has this property is given as follows:

$$\hat{d}_i = e^{\varrho(K_{\mathrm{dB}} - z_i) - \varrho^2(\alpha+\sigma^2)}. \tag{7}$$

where $\varrho \triangleq \frac{1}{\zeta n_{\mathrm{PL}}}$. In this section, we first mathematically characterize the estimation error covariance matrix of this LS estimator when considering the probabilistic channel modeling of Section II and in the presence of multipath fading and correlated shadowing. We then find the impact of the underlying channel parameters and measurement positions on the estimation performance of this estimator. We have,

$$C_{\mathrm{LS}}(\mathcal{Q}, q_b) = (A^T A)^{-1} A^T C_b A (A^T A)^{-1}, \tag{8}$$

where C_b denotes the covariance matrix of b. In order to find C_b, we need to calculate $\mathbb{E}\{\hat{d}_i^4\}$ and $\mathbb{E}\{\hat{d}_i^2\hat{d}_j^2\}$, for all $i, j \neq i$. We have

$$\mathbb{E}\{\hat{d}_i^4\} = e^{4K_{\mathrm{dB}}\varrho - 4\varrho^2(\alpha+\sigma^2)}\mathbb{E}\{e^{-4\varrho z_i}\} = e^{4\varrho^2(\alpha+\sigma^2)}d_i^4. \tag{9}$$

To calculate $\mathbb{E}\{\hat{d}_i^2\hat{d}_j^2\}$, however, the distribution of z_j conditioned on z_i needs to be characterized. We can easily confirm that the pdf of z_j, conditioned on z_i and the channel parameters is given by a Gaussian distribution with mean $K_{\mathrm{dB}} - n_{\mathrm{PL}}D_j(q_b) + \frac{\alpha}{\alpha+\sigma^2}e^{-\frac{\|q_i - q_j\|}{\beta}}\big(z_i - K_{\mathrm{dB}} + n_{\mathrm{PL}}D_i(q_b)\big)$ and variance $\alpha + \sigma^2 - \frac{\alpha^2}{\alpha+\sigma^2}e^{-2\frac{\|q_i - q_j\|}{\beta}}$, where $D_j(q_b) = 10\log_{10}\|q_j - q_b\|$ (see Section II of [7] for more details). After some straightforward calculations, we obtain

$$\begin{aligned}\mathbb{E}\{\hat{d}_i^2\hat{d}_j^2\} &= e^{4K_{\mathrm{dB}}\varrho - 4\varrho^2(\alpha+\sigma^2)}\mathbb{E}\{e^{-2\varrho(z_i+z_j)}\}\\ &= e^{4K_{\mathrm{dB}}\varrho - 4\varrho^2(\alpha+\sigma^2)}\mathbb{E}_{z_i}\Big\{e^{-2\varrho z_i}\mathbb{E}_{z_j}\{e^{-2\varrho z_j}|z_i\}\Big\}\\ &= e^{4\varrho^2\alpha e^{-\frac{\|q_i - q_j\|}{\beta}}}d_i^2 d_j^2.\end{aligned} \tag{10}$$

Let us define $\Upsilon_{k\times k}$ with $[\Upsilon]_{i,j} = e^{4\varrho^2[R_{\mathrm{tot},\mathcal{Q}}]_{i,j}} - 1$. Consider the following decomposition of Υ:

$$\Upsilon = \begin{bmatrix}\delta_{1\times 1} & \varphi_{k-1\times 1}^T\\ \varphi_{k-1\times 1} & \Delta_{k-1\times k-1}\end{bmatrix}. \tag{11}$$

The covariance matrix of the vector b can be then rewritten as

$$C_b = \delta d_1^4 1_{k-1}1_{k-1}^T + \Gamma\Delta\Gamma - d_1^2\Gamma 1_{k-1}\varphi^T - d_1^2\varphi 1_{k-1}^T\Gamma, \tag{12}$$

where $\Gamma = \mathrm{diag}[d_2^2 \cdots, d_k^2]$. Next, we investigate the impact of the underlying channel parameters on the LS estimation of the transmitter position.

A. Impact of the Underlying Channel Parameters and Sampling Positions on the Error Covariance of the LS Estimator

The next theorem characterizes the impact of the channel parameters on $C_{\mathrm{LS}}(\mathcal{Q}, q_b)$:

Theorem IV.1. *Without loss of generality, consider the case that the transmitter is located at the origin. Assume there exists* $q^* = [\rho\cos(\phi), \rho\sin(\phi)]^T \in \mathcal{W}$ *such that* $\|q_i - q^*\| \ll \rho\ \forall i$. *We then have the following properties: 1)* $\mathrm{trace}\{C_{\mathrm{LS}}(\mathcal{Q}, q_b)\}$

is independent of K_{dB} and a decreasing function of n_{PL}; 2) $\mathrm{trace}\{C_{LS}(\mathcal{Q},q_b)\}$ is an increasing function of α and σ^2; 3) if $\frac{\|q_i-q_j\|^2}{\beta^2} \ll 1\ \forall i,j$, $\mathrm{trace}\{C_{LS}(\mathcal{Q},q_b)\}$ is a decreasing function of β.

Proof: Under the assumption that $\|q_i - q^*\| \ll \rho\ \forall i$, we have $d_i \approx \rho\ \forall i$. Hence,

$$C_b \approx \rho^4\Big(\delta 1_{k-1}1_{k-1}^T + \Delta - 1_{k-1}\varphi^T - \varphi 1_{k-1}^T\Big) \quad (13)$$
$$= \rho^4 \begin{bmatrix}1_{k-1} & -I_{k-1}\end{bmatrix}\begin{bmatrix}\delta & \varphi_{k-1\times 1}^T \\ \varphi_{k-1\times 1} & \Delta_{k-1\times k-1}\end{bmatrix}\begin{bmatrix}1_{k-1}^T \\ -I_{k-1}\end{bmatrix}.$$

As can be seen, C_b is not a function of K_{dB}. We also have $\frac{d}{dn_{\mathrm{PL}}}[\Upsilon]_{i,j} = -\frac{2\ln^2(10)}{25n_{\mathrm{PL}}^3}[R_{\mathrm{tot},\mathcal{Q}}]_{i,j}e^{4\varrho^2[R_{\mathrm{tot},\mathcal{Q}}]_{i,j}}$. Therefore, $\frac{d}{dn_{\mathrm{PL}}}\Upsilon = -\frac{2\ln^2(10)}{25n_{\mathrm{PL}}^3}R_{\mathrm{tot},\mathcal{Q}} \circ \big(\Upsilon + 1_k1_k^T\big)$, where $\circ$ denotes the Hadamard product. Since $R_{\mathrm{tot},\mathcal{Q}}$ and $\Upsilon + 1_k1_k^T$ are both positive definite matrices, from Theorem 7.5.3 of [15] it can be confirmed that $\frac{d}{dn_{\mathrm{PL}}}\Upsilon \prec 0$. Thus, $\frac{d}{dn_{\mathrm{PL}}}C_b \preceq 0$. Let $e_1 = [1,0]^T$ and $e_2 = [0,1]^T$ denote unit vectors in $\mathbb{R}^2$. We then have $\frac{d}{dn_{\mathrm{PL}}}\mathrm{trace}\big\{C_{\mathrm{LS}}(\mathcal{Q},q_b)\big\} = \sum_{i=1}^2 e_i^T(A^TA)^{-1}A^T\frac{d}{dn_{\mathrm{PL}}}C_bA(A^TA)^{-1}e_i \le 0$.

In order to show that $\mathrm{trace}\big\{C_{\mathrm{LS}}(\mathcal{Q},q_b)\big\}$ is an increasing function of α, it suffices to show that $\frac{d}{d\alpha}\Upsilon \succ 0$. We have $\frac{d}{d\alpha}[\Upsilon]_{i,j} = 4\varrho^2[R_{\mathrm{norm},\mathcal{Q}}]_{i,j}e^{4\varrho^2[R_{\mathrm{tot},\mathcal{Q}}]_{i,j}}$. Since $R_{\mathrm{norm},\mathcal{Q}}$ and $\Upsilon + 1_k1_k^T$ are both positive definite matrices, similarly we can show that $\frac{d}{d\alpha}\Upsilon \succ 0$, which results in $\frac{d}{d\alpha}\mathrm{trace}\{C_{\mathrm{LS}}(\mathcal{Q},q_b)\} \ge 0$. Furthermore, we have $\frac{d}{d\sigma^2}C_b = 4\varrho^2e^{4\varrho^2(\alpha+\sigma^2)}\big(1_k1_k^T + I_K\big) \succ 0$, which implies that $\mathrm{trace}\big\{C_{\mathrm{LS}}(\mathcal{Q},q_b)\big\}$ is an increasing function of σ^2. Next we prove the third property. Under the assumption that $\frac{\|q_i-q_j\|^2}{\beta^2} \ll 1$ for $1 \le i,j \ne i \le k$, we have $[\Upsilon]_{i,j} = e^{4\varrho^2\alpha e^{-\frac{\|q_i-q_j\|}{\beta}}} - 1 \approx e^{4\varrho^2\alpha} - 1 - 4\varrho^2\alpha e^{4\varrho^2\alpha}\frac{\|q_i-q_j\|}{\beta}$. Therefore, we have, $\frac{d}{d\beta}[\Upsilon]_{i,j} \approx \frac{1}{\beta^2}4\varrho^2\alpha e^{4\varrho^2\alpha}\|q_i - q_j\|$ for $1 \le i,j \le k$. Let $T_{\mathcal{Q}'}$ represent the distance matrix corresponding to $\mathcal{Q}'$, where $\mathcal{Q}' = \{q_2,\cdots,q_k\}$. We have $[T_{\mathcal{Q}'}]_{i,j} = \|q_{i+1} - q_{j+1}\|$. Define $\zeta_{\mathcal{Q}'}(q_1) \triangleq \big[\|q_2-q_1\|,\cdots,\|q_k-q_1\|\big]^T$. We then have, $\frac{d}{d\beta}C_b = \frac{\rho^4}{\beta^2}4\varrho^2\alpha e^{4\varrho^2\alpha}\Big[T_{\mathcal{Q}'} - 1_{k-1}\zeta_{\mathcal{Q}'}^T(q_1) - \zeta_{\mathcal{Q}'}(q_1)1_{k-1}^T\Big]$. In Theorem 4 of [7], we utilized several properties of Euclidean distance matrices and showed that $1_{k-1}\zeta_{\mathcal{Q}'}^T(q_1) + \zeta_{\mathcal{Q}'}(q_1)1_{k-1}^T - T_{\mathcal{Q}'}$ is positive-semidefinite. Therefore, we have $\frac{d}{d\beta}C_b \preceq 0$ for sufficiently large values of β, which completes the proof. ■

Remark IV.1. *Consider the scenario of Theorem IV.1. From (13), we have $C_b\big|_{\beta=0} = (e^{4\varrho^2(\alpha+\sigma^2)} - 1)\rho^4(1_k1_k^T + I_k)$ and $C_b\big|_{\beta=\infty} = (e^{4\varrho^2(\alpha+\sigma^2)} - e^{4\varrho^2\alpha})\rho^4(1_k1_k^T + I_k)$. Therefore, $C_b\big|_{\beta=0} \succeq C_b\big|_{\beta=\infty}$, which results in $C_{LS}(\mathcal{Q},q_b)\big|_{\beta=0} \succeq C_{LS}(\mathcal{Q},q_b)\big|_{\beta=\infty}$.*

Fig. 1 shows the impact of β on $\mathrm{trace}\big\{C_{\mathrm{LS}}(\mathcal{Q},q_b)\big\}$. In this example, the transmitter is located at $q_b = [0,0]^T$. The robot takes $k = 10$ measurements randomly in a 1 m by 1 m square neighborhood of $[10,10]$. As can be seen for small values of β, i.e. $\beta < 0.3$m, the estimation error of the transmitter

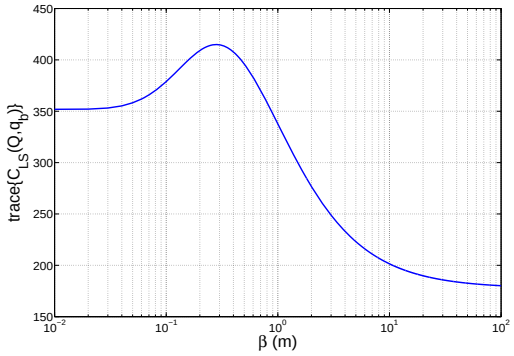

Fig. 1: impact of β on the estimation error of the transmitter position in the LS approach.

position is an increasing function of β. However, as β is becoming sufficiently large compared to the distance between the measurements, $\mathrm{trace}\big\{C_{\mathrm{LS}}(\mathcal{Q},q_b)\big\}$ becomes a decreasing function of β, as shown in Theorem IV.1.

We next investigate the impact of the sampling positions on the estimation quality of the LS approach. The next theorem shows that as a fixed constellation of channel measurements moves towards the transmitter, $\mathrm{trace}\big\{C_{\mathrm{LS}}(\mathcal{Q},q_b)\big\}$ decreases. We utilize this property in Section V when introducing our motion planning strategy.

Theorem IV.2. *Let $\mathcal{Q} = \{q_1,q_2,\cdots,q_k\}$ and $\mathcal{Q}' = \{q_1',q_2',\cdots,q_k'\}$ represent two sets of measurement positions such that $q_i' = q_i + q_{dis}$ and $d_i' \le d_i$ for $1 \le i \le k$, where q_{dis} denotes the fixed displacement vector and $d_i' = \|q_i' - q_b\|$. Then, if $\beta \to 0$ (uncorrelated channel), $\mathrm{trace}\big\{C_{LS}(\mathcal{Q}',q_b)\big\} \le \mathrm{trace}\big\{C_{LS}(\mathcal{Q},q_b)\big\}$.*

Proof: Define $\Gamma' \triangleq \mathrm{diag}\big[{d_2'}^2,\cdots,{d_k'}^2\big]$. Under the assumption of $\beta = 0$, we have $C_b' = (e^{4\varrho^2(\alpha+\sigma^2)} - 1)\big({d_i'}^4 1_{k-1}1_{k-1}^T + \Gamma'^2\big)$. Since $d_i' \le d_i$ it can be easily confirmed that $C_b' \preceq C_b$. On the other hand, if $q_i' = q_i + q_{\mathrm{dis}}$, we then have $[U']_i = x_i' - x_1' = x_i - x_1 = [U]_i$ and similarly $V' = V$, which results in $C_{\mathrm{LS}}(\mathcal{Q}',q_b) \preceq C_{\mathrm{LS}}(\mathcal{Q},q_b)$. ■

One of the disadvantageous of the lateration-based LS estimator is the sensitivity to the relative positions of the measurements. Next theorem shows the resulting impact of the number of the sampling positions on the estimation error of the transmitter position.

Theorem IV.3. *The estimation error variance of the transmitter position in the LS approach depends on the sampling positions and it is not necessarily a decreasing function of the number of measurements.*

Proof: We skip the proof due to page limit. ■

Theorem IV.3 implies that the lateration-based LS estimator does not necessarily result in a better estimation quality as we take more measurements. For instance, consider the scenario where two samples are taken from the workspace randomly. If the third sample is taken on a line which passes through the first two samples, then matrix A would not be full rank, which degradates the estimation quality drastically. Therefore,

the relative position of the samples should be chosen wisely, as explained in the next section.

V. Motion planning for Improving the Transmitter Localization Performance

In the previous sections, we studied two approaches for transmitter localization in wireless sensor networks. More specifically, we characterized the effects of the underlying channel parameters as well as sampling positions on the localization performance of both approaches. Consider the case, where a number of mobile robots gather a number of channel measurements along their trajectories and estimate the transmitter position based on these measurements. Obviously, the trajectories of the robots affect the transmitter localization performance, as both the CRLB of (3) and estimation error covariance of (8) are functions of the positions of the channel measurements. A natural question is then as follows: how can we design the trajectory for a mobile robot such that the collected channel measurements along the trajectory result in the best estimate of the transmitter location at the end of the operation? Next, we look at the implication of the previous analysis for such a motion optimization, based on a greedy sub-optimal approach, in order to improve the localization performance.

Assume that a mobile robot estimates the position of a transmitter in the workspace $\mathcal{W}$ using the gathered samples along its trajectory. Let $\mathcal{Q}_t = \{q_{t-k_w+1}, \cdots, q_t\} \subset \mathcal{W}$ represent the set of last k_w channel measurement positions along the trajectory of the robot up to time t, where q_t denotes the position of the robot at time t and k_w represents the *window size*. Let $\Psi(\mathcal{Q}_t, q_b)$ denote a measure of uncertainty when the transmitter position is estimated using the measurements in $\mathcal{Q}_t$. In this section, we consider the following uncertainty measures:

1) CRLB-based motion planning:

$$\Psi(\mathcal{Q}_t, q_b) \triangleq \operatorname{trace}\left\{J^{-1}(\mathcal{Q}_t, q_b)\right\}. \tag{14}$$

2) LS-based motion planning:

$$\Psi(\mathcal{Q}_t, q_b) \triangleq \operatorname{trace}\left\{C_{\mathrm{LS}}(\mathcal{Q}_t, q_b)\right\}. \tag{15}$$

Let $\hat{q}_{b,t}$ denote the estimate of the mobile robot at time t using its last k_w channel measurements. Note that in the CRLB approach, we use the ML estimator of (2) in order to estimate the transmitter position in each step. On the other hand, for the LS-based motion planning of (15), we use the LS estimator of (6) in each step. Assume a mobile robot with the following discrete-time holonomic dynamics:

$$q_{t+1} = q_t + u_t, \qquad \|u_t\| \le u_{\max}, \tag{16}$$

where u_t is the control input of the robot at time t and $u_{\max}$ is its maximum step size. We can then find the next position of the robot by minimizing the uncertainty measure at time $t+1$. We have the following motion optimization problem to find the next best position of the robot at time t:

$$q^*_{t+1} = \underset{q_{t+1}}{\operatorname{argmin}}\ \Psi\big(\mathcal{Q}_t \cup \{q_{t+1}\}, \hat{q}_{b,t}\big)$$
$$\text{s.t. } 1)\ q_{t+1} = q_t + u_t,\ 2)\ \|u_t\| \le u_{\max},\ 3)\ q_{t+1} \in \mathcal{V}_t, \tag{17}$$

where the time-varying set $\mathcal{V}_t$ is defined as follows:

$$\mathcal{V}_t \triangleq \left\{ q \in \mathcal{W} \;\middle|\; \frac{(q-q_t)^{\mathrm{T}}(\hat{q}_{b,t}-q_t)}{\|q-q_t\|\|\hat{q}_{b,t}-q_t\|} > \varepsilon \right\}, \tag{18}$$

for a given $0 < \varepsilon < 1$. By selecting the next position of the robot from $\mathcal{V}_t$, we guarantee that the robot moves within a cone which points towards the current estimate of the transmitter position. Note that this constraint improves the estimation quality, specially when the robot is far enough from the transmitter (see Theorem III.2 and Theorem IV.1). However, this constraint can be released as the robot becomes closer to the transmitter.

The LS approach is a geometric-based approach and is not statistically optimum. Therefore, more samples would not necessarily result in a better estimation quality (as we showed in Theorem IV.3). Furthermore, the newer channel measurements are more informative for localization purposes. This explains why we choose to use a window size. Note that the window size can also reduce the computational complexity. We also assume that the robot collects a number of a priori measurements before it starts the motion optimization.

VI. Simulation results

In this section, we present our simulation results for localizing a transmitter using a mobile robot. The workspace is a 100m by 100m square, where the transmitter is located at position $q_b = [50, 50]$ m. The received signal strength $\Upsilon_{\mathrm{dB}}(q)$ is generated using our probabilistic channel simulator [16] with the following channel parameters: $K_{\mathrm{dB}} = -10$ dB, $n_{\mathrm{PL}} = 2$, $\sqrt{\alpha} = 2$ dB and $\sigma = 0.87$ dB. In order to show the effects of the channel correlation, we simulate two channels with $\beta = 0$ (uncorrelated), $\beta = 20$ m (highly correlated). The rest of the parameters are chosen as follows: $k_w = 20$, $\varepsilon = \frac{\sqrt{3}}{2}$, $u_{\max} = 5$ m.

Fig. 2 shows the trajectory of the robot after using the motion planning strategy of (17). The upper and lower rows correspond to the cases where CRLB-based and LS-based motion planning approaches are used, respectively. From left to right, the channels experience a shadowing component with $\beta = 0$ and $\beta = 20$ m, respectively. In all the figures, the trajectory of the robot is superimposed on a plot of the RSS. The empty boxes and the filled ones in the figures also denote the initial and final positions of the robot, respectively. Fig. 3 compares the time evolution of the uncertainty measure of both CRLB and LS approaches for the two cases of $\beta = 0$ and $\beta = 20$ m. Note that for the CRLB-based approach, the transmitter position is estimated using an ML estimator in each time step. For further comparison, we also simulated the case where a random trajectory is used for the robot in both ML and LS approaches. In the random trajectory case, the time evolution of $\Psi(\mathcal{Q}_t, q_b)$ is plotted after averaging over

50 different trajectories. Unlike the optimal case, however, all the collected channel measurements are used in the estimation process (or equivalently k_w is selected very large) in this case. Also, the case of Random (ML) refers to the case where the transmitter position is estimated using the ML estimator of (2) at every step.

For the optimized CRLB and LS approaches, Fig. 2 shows that the robot reaches the transmitter after some times. The mobile robot in the LS-based approach, however, moves towards the transmitter less smoothly than in the CRLB-based approach. Another observation is that in Fig. 3 the asymptotic performance of both CRLB and LS approaches are better in the right figure than in the left one. For instance, the estimation performance of the LS-based approach after 80s is 7dB better in the case of $\beta = 20$ as compared to the case of $\beta = 0$. This is due to the fact that the performance of transmitter localization improves for very large β, as explained previously. Finally, by comparing the performance to the case of random trajectories, it can be seen that optimizing the trajectory based on the CRLB or LS approaches, can improve the transmitter localization performance considerably.

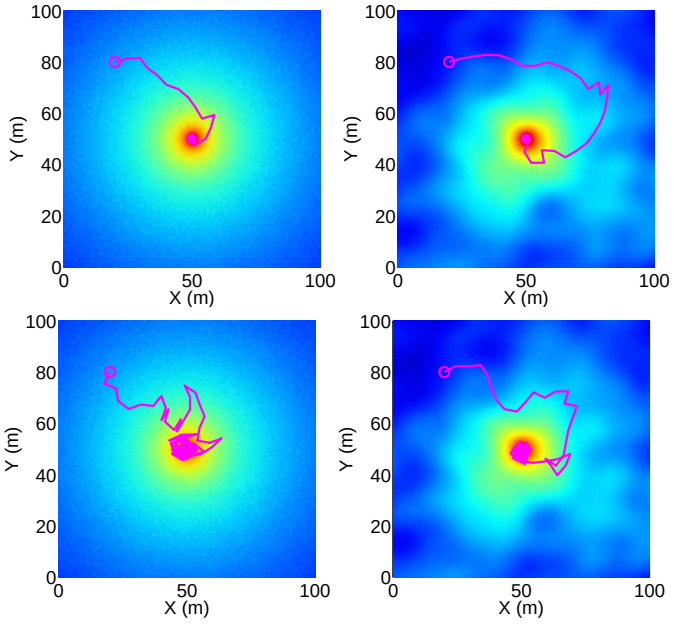

Fig. 2: The trajectory of the robot after using the motion planning strategy of (17). The upper and lower rows correspond to the cases where CRLB and LS approaches are used, respectively. From left to right, the channels experience a shadowing component with $\beta = 0$ and $\beta = 20$ m, respectively.

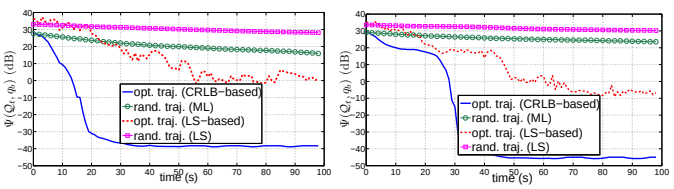

Fig. 3: Time evolution of $\Psi(\mathcal{Q}_t, q_b)$ for both CRLB and LS approaches for the two cases of $\beta = 0$ (left) and $\beta = 20$ m (right).

VII. Conclusion

In this paper, we studied the problem of localizing a transmitter position using the probabilistic model of channel variations in a networked robotic operation. We considered the Cramer-Rao lower bound (CRLB) of the localization error as well as the error covariance matrix of a least square (LS) estimator. We then mathematically analyzed the impact of the positions of the channel measurements as well as the underlying channel parameters, such as shadowing power, correlation distance, multipath power, and path loss slope, on the localization performance. Motivated by our analysis, we then utilized a motion planning strategy in order to improve the localization performance. Our simulation results confirmed the theoretical analysis.

References

[1] J. Reich, V. Misra, D. Rubenstein, and G. Zussman, "Connectivity maintenance in mobile wireless networks via constrained mobility," *IEEE Journal on Selected Areas in Communications,*, vol. 30, pp. 935 –950, june 2012.

[2] Y. Yan and Y. Mostofi, "Robotic Router Formation - A Bit Error Rate Approach," in *Proceedings of the 29th IEEE Military Communications Conference (Milcom)*, (San Jose, CA), pp. 1287–1292, November 2010.

[3] K. Lorincz, D. Malan, T. Fulford-Jones, A. Nawoj, A. Clavel, V. Shnayder, G. Mainland, M. Welsh, and S. Moulton, "Sensor networks for emergency response: challenges and opportunities," *IEEE Pervasive Computing*, vol. 3, pp. 16 – 23, oct.-dec. 2004.

[4] A. J. Weiss, "Direct position determination of narrowband radio frequency transmitters," 2004.

[5] A. Wadhwa, U. Madhow, J. P. Hespanha, and B. M. Sadler, "Following an RF trail to its source," in *Proc. of the 49th Annual Allerton Conf. on Comm., Contr., and Computing*, Sep. 2011.

[6] J. Fink and V. Kumar, "Online methods for radio signal mapping with mobile robots," in *IEEE International Conference on Robotics and Automation*, pp. 1940–1945, 2010.

[7] M. Malmirchegini and Y. Mostofi, "On the spatial predictability of communication channels," *IEEE Transactions on Wireless Communications*, vol. 11, pp. 964 –978, march 2012.

[8] Y. Mostofi, M. Malmirchegini, and A. Ghaffarkhah, "Estimation of communication signal strength in robotic networks," in *Proceedings of IEEE International Conference on Robotics and Automation*, pp. 1946 –1951, May 2010.

[9] A. Ghaffarkhah and Y. Mostofi, "Communication-aware motion planning in mobile networks," *IEEE Transactions on Automatic Control*, vol. 56, pp. 2478 –2485, oct. 2011.

[10] A. Goldsmith, *Wireless Communications*. Cambridge University Press, 2005.

[11] W. C. Jakes, *Microwave Mobile Communications*. New York: Wiley-IEEE Press, 1994.

[12] J. Yang and Y. Chen, "Indoor localization using improved rss-based lateration methods," in *IEEE Global Telecommunications Conference, 2009.*, dec. 2009.

[13] F. Seco, A. Jimenez, C. Prieto, J. Roa, and K. Koutsou, "A survey of mathematical methods for indoor localization," in *IEEE International Symposium on Intelligent Signal Processing, 2009. WISP 2009.*, pp. 9 –14, aug. 2009.

[14] F. Thomas and L. Ros, "Revisiting trilateration for robot localization," *IEEE Transactions on Robotics*, vol. 21, pp. 93 – 101, feb. 2005.

[15] R. Horn and C. Johnson, *Matrix Analysis*. New York: Cambridge University Press, 1999.

[16] A. Gonzalez-Ruiz, A. Ghaffarkhah, and Y. Mostofi, "A comprehensive overview and characterization of wireless channels for networked robotic and control systems," *accepted to appear in Journal of Robotics*, 2012.